

Article

Application of Phase-Shifting Transformer with Longitudinal and Transverse Voltage Regulation

Paweł Albrechtowicz ¹, Bartosz Rozegnał ¹, Jerzy Szczepanik ¹, Maciej Sułowicz ^{1,*} and Piotr Cisek ²

¹ Department of Electrical Engineering, Cracow University of Technology, Warszawska 24 St., 31-155 Cracow, Poland; pawel.albrechtowicz@pk.edu.pl (P.A.); bartosz.rozegnal@pk.edu.pl (B.R.); jerzy.szczepanik@pk.edu.pl (J.S.)

² Department of Energy, Cracow University of Technology, 31-864 Cracow, Poland; piotr.cisek@pk.edu.pl

* Correspondence: maciej.sulowicz@pk.edu.pl

Abstract: This article was written to present a new solution for a phase-shifting transformer and to show that, in many aspects, the proposed device is more functional and improved when compared to the other currently available phase-shifting structures. The article shows the construction of the new phase-shifting transformer, with longitudinal and transverse voltage regulation. The proposed device's functionality and available operation states are compared to other existing solutions. Selected steady-state variants of the operation of the proposed transformer were checked based on computer simulations and the laboratory model presented in detail in the article. Convergence between measurements and simulations was achieved. Power flow calculations were also performed in the five-node electrical power system model. In these calculations, two variants of the proposed device's work were considered and compared with the asymmetric phase shifter. The tests confirmed in the proposed structure, both angle and voltage regulation, enabled maintaining a constant active power flow. The authors show that the proposed solution combines the advantages and functionality of various types of phase shifters while, at the same time, being characterized by a much simpler structure, which results in a two-times-lower cost of the device.

Keywords: phase shifters; phase-shifting transformers; power flows; control of power flow; smart grid; power system; FACTS



Citation: Albrechtowicz, P.; Rozegnał, B.; Szczepanik, J.; Sułowicz, M.; Cisek, P. Application of Phase-Shifting Transformer with Longitudinal and Transverse Voltage Regulation. *Energies* **2023**, *16*, 4603. <https://doi.org/10.3390/en16124603>

Academic Editor: Sérgio Cruz

Received: 30 April 2023

Revised: 27 May 2023

Accepted: 5 June 2023

Published: 8 June 2023



Copyright: © 2023 by the authors. Licensee MDPI, Basel, Switzerland. This article is an open access article distributed under the terms and conditions of the Creative Commons Attribution (CC BY) license (<https://creativecommons.org/licenses/by/4.0/>).

1. Introduction

An increase in the distributed energy resources (DERs) in power systems changes the well-known models of the power flows, where the energy is transmitted in a steady state (slow rate changes) from conventional electric plants via transmission lines to HV substations. Then, via distribution lines, energy is delivered to consumers. Nowadays, the DERs force flows from distribution lines to transmission ones and, therefore, the most critical changes in the power flows occur via the direction of the energy transmission [1]. The main problem associated with the large penetration of DERs is balancing energy production and the achievement of global stability of the power system, which was analyzed in [2]. Global system stability requires effective management of the distributed systems. These challenges are called DER management systems (DERMSs), proposed in [3] as an effective software tool.

To achieve effective power flow control in the power systems, several different control devices, such as phase-shifting transformers (PSTs), unified power flow controllers (UPFCs), interconnection power flow controllers (IPFCs) and other FACTS (Flexible Alternating-Current Transmission Systems) devices, are installed.

PSTs have been widely used in different regions of the world to control power flow between country power systems, e.g., in Europe (Germany—Poland [4,5], the Benelux region [6,7], Italy—Slovenia [8]), in India [9] or in the USA [10]. Apart from existing units,

the next ones are under construction or planned to be installed in power systems [11]. According to a publication [12], at the beginning of this century, in Europe, PSTs with total power equal to 5 GW were installed, while in 2030, it is predicted that the total power of PSTs installed will be 50 GW. Therefore, there is still a need to develop these units to achieve the best properties or to attain proposals for new applications. In the literature, a new concept of power flow regulating devices, which are dedicated to medium-voltage (MV) or low-voltage (LV) systems, can be found. In [13], the authors propose a transformer-thyristor solid-state device called the power flow control device (PFCD). This device can be applied to MV distribution systems to control both voltage and power flows. At the LV level, the idea of additional series voltage to regulate network parameters is adopted (Inline Power Regulator—IPR) [14].

In reference [15], the authors research how the PST may influence power flows in the Bosnia and Herzegovina distribution system, including the connected subsystems. They conclude that PST has a positive impact and is an important device to control power flows and to increase stability and operational safety. PSTs with thyristor-controlled systems, which were tested in [16], can be an efficient tool used to increase dynamic stability during disturbances in the system.

The optimal power flow issue was analyzed in [17]. The authors claimed that using PST can affect the technical and economic aspects of the power system functioning. In turn, publication [18] adopted particle swarm optimization to achieve the best results of the PST's settings to minimize unscheduled power flows. A positive impact on the power system functioning, taking into account the optimal size and place of the PST installation, was presented in [19].

This manuscript proposes using an asymmetric PST (APST), which provides regulation of both longitudinal and transverse voltages (additional, series). Transverse voltage is injected into the line. The possibility of both voltage regulation situations allows for better voltage values and direction properties. The proposed regulation of longitudinal voltage is a way to eliminate the main disadvantage of classical APST—an output voltage growth in relation to APST input voltage [20]. Similar units have been known for years. They were analyzed in the coupling of the 400 and 220 kV power systems to regulate both voltage levels and the phase angles of the systems [21]. However, their role in the system differed from those proposed in this article.

An interesting unit that allows one to achieve high flexibility in the regulation process is the Sen Transformer. As stated in reference [22], this device can be compared to UPFC, and its properties can be even better, while the price and size are much lower than UPFC. The Sen Transformer details are available in patents: [23,24].

A complex control system or a complicated structure characterizes the mentioned solutions. All this contributes to the generally high costs of implementing the solution. On the other hand, a particular drawback of the proposed system is the need to use two transformers for the construction, which results in increased losses occurring during the operation of the device.

The main goal of this publication is to present the impact of APST on the power flows, voltages and angles in the testing IEEE five-bus system. The research will consider classical APST and modified APST with longitudinal and transverse voltage regulation. This APST unit is called an asymmetric controllable phase-shifting transformer (ACPST). In the scientific literature, there is no information about similar devices. Therefore, this article may fill a research gap and lead to more flexible applications based on traditional elements, such as transformers. The research examples mentioned above are aimed at finding optimal PST settings, and almost as standard, they are usually based on the symmetric PST (SPST) or the thyristor-controlled PST. ACPST may open new directions in such research.

In Section 2, the manuscript describes the properties of PSTs with highlighted testing proposed ACPST construction. The following paragraph presents a researched model of the power system. The laboratory results are presented in Section 4. Section 5 presents the

power flow calculations in five-bus power systems. Section 6 contains the conclusions from tests performed during the research.

2. APST and ACPST Description

The theory of the PST has been known for many years. Considering classical asymmetric PSTs, the most essential issue refers to the output and input voltage dependency. The output voltage in APST (U_{out}) is always greater than or equal to the input one (U_{in}).

This APST feature is a consequence of the quadrature voltage injection. Figure 1 presents a phasor diagram of the input (U_S), quadrature (ΔU), output voltages (U_L) and introduced phase angle α .

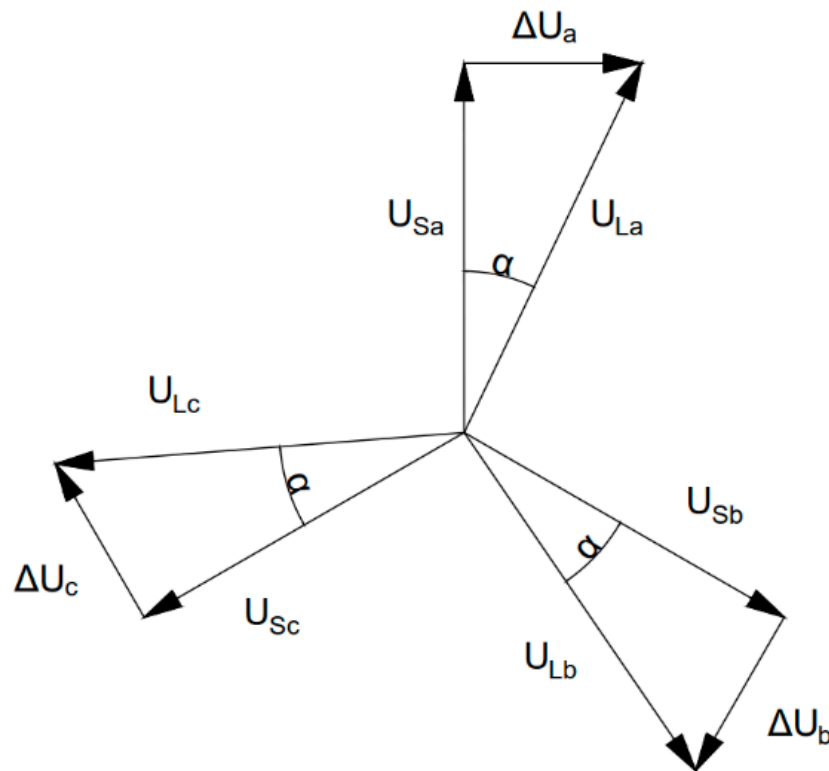


Figure 1. APST phasor diagram.

Active power flowing through the transmission line is given as:

$$P = \frac{U_R}{X + X_{PST}} (U_S \sin \delta + \Delta U \cos \delta) \tag{1}$$

where: U_R —receiving-end voltage, (V); U_S —sending-end voltage (V); X —line reactance, (Ω); X_{PST} —PST series reactance, (Ω); δ —natural line phase angle, ($^\circ$).

It should be noted that in considered high-voltage (HV) or extra-high-voltage (EHV) cases, the line reactance to resistance ratio is even greater than 10, so in the approximate analyses, the line resistance can be omitted [25,26].

Modifying classic APST by introducing not only (series) transverse voltage regulation but also the longitudinal one allows one to achieve better properties and a wider range of possible operating states. The three-phase phasor diagram for ACPST is shown in Figure 2.

The relation between U_S and U'_S is given as the extra transformer (ET—see Figure 6) ratio η :

$$\eta = \frac{U_S}{U'_S} \tag{2}$$

Based on the proposed PST’s principal properties, possible work states can be highlighted (Figure 3).

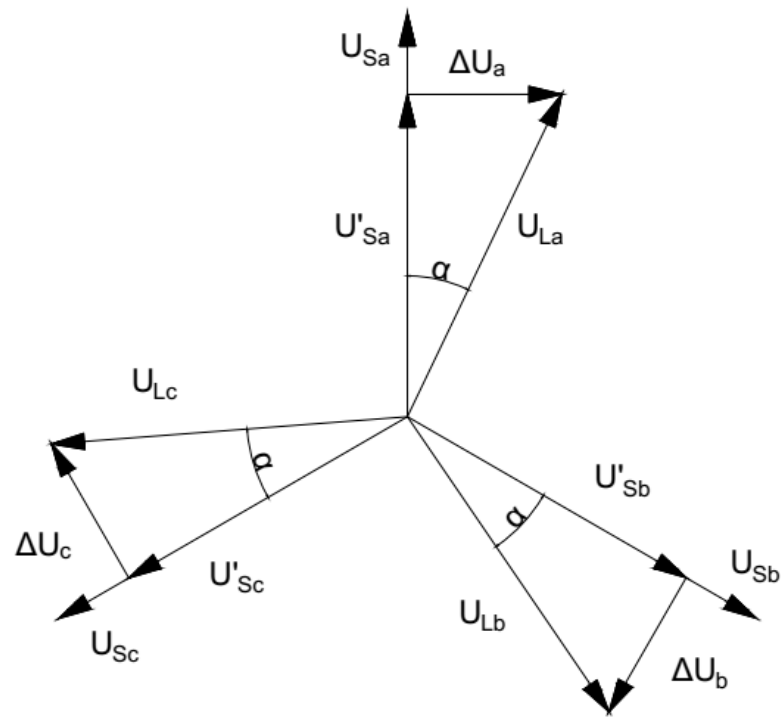


Figure 2. ACPST phasor diagram for lowered longitudinal input voltage.

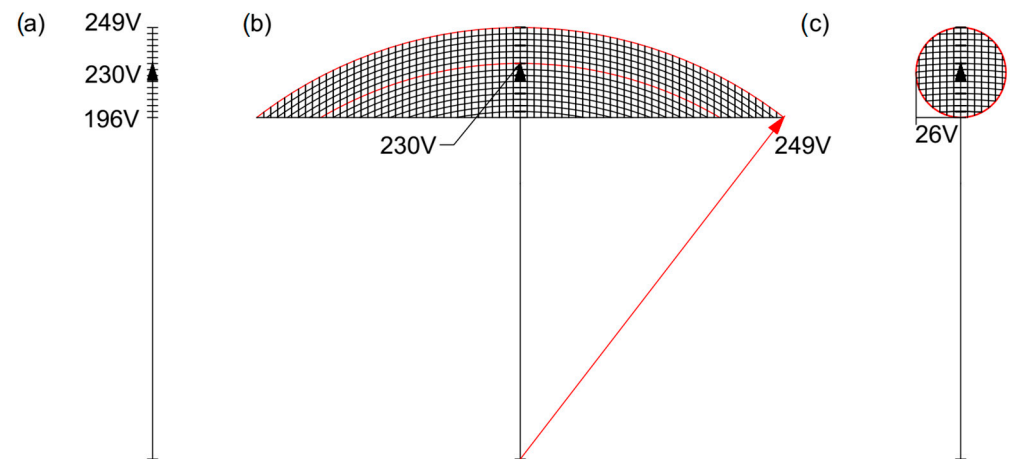


Figure 3. Chosen ACPST’s operation states: (a) only longitudinal voltage regulation—like a classic transformer, (b) constant output voltage value for its different angles, (c) a circle of possible voltage values like in UPFC.

Figure 3 represents the chosen ACPST output voltage and angle control. As mentioned, the APST output value is always greater than the input one when additional transverse voltage is different from 0 ($\Delta U \neq 0$). In ACPST, a wide range of possible control strategies can be used, e.g., the classical step up/down transformer (an equivalent of tap changer voltage adjustment—Figure 3a), the quasi-symmetrical PST (the same input and output voltage value with changed angle—Figure 3b) or the UPFC, able to add voltage to obtain any state inside the red circle (Figure 3c). Obviously, ACPST can function as an APST, so four possible control strategies can be seen within one device. This is a great advantage in

comparison to APST or SPST. The active power transfer through the line for the ACPST application can be expressed as:

$$P = \frac{U_R}{X + X_{PST}} \left(\frac{U_S}{\eta} \sin\delta + \Delta U \cos\delta \right) \quad (3)$$

According to Formula (3), the active power transfer in ACPST can also be managed by longitudinal voltage regulation [27]. Proper selection of parameters η and ΔU allows one to find any of the control strategies shown in Figure 3.

The theoretical active power flows and introduced angles α for different input voltages are presented in Figures 4 and 5.

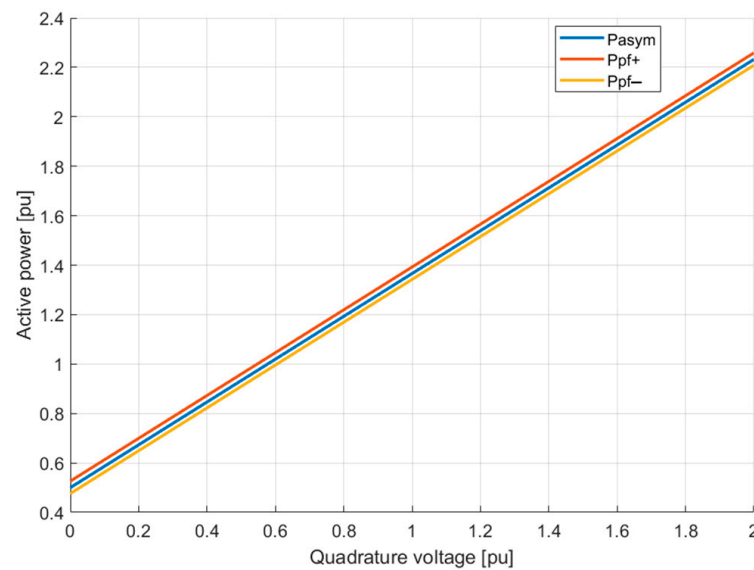


Figure 4. ACPST active power flow for longitudinal voltages: 95% Un (yellow), Un (blue), 105% Un (red).

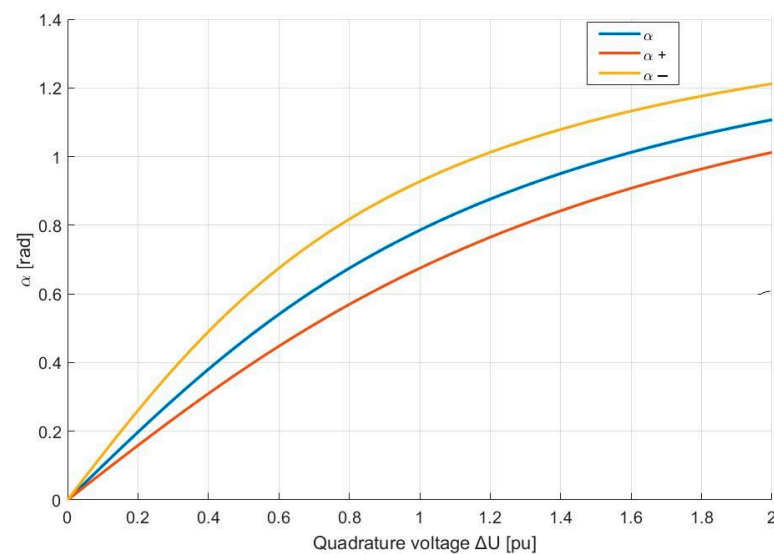


Figure 5. ACPST angle α range for longitudinal voltages: 95% Un (yellow), Un (blue), 105% Un (red).

When the longitudinal voltage is lowered, the transmitted power is smaller, while the angle α is greater. Reverse dependency is observed for higher longitudinal voltage; however, both rules are consistent with the expected ACPST work.

3. Materials and Methods

3.1. Laboratory Setup

To prepare for laboratory research, the testing ACPST was arranged. In the LV laboratory power system, a two-transformer ACPST was introduced. The data for both transformers are presented in Table 1.

Table 1. Transformers' data.

	Series Transformer ST	Extra Transformer ET
Rated Primary Voltage, V	3×400	3×400
Rated Secondary voltage, V	$3 \times 128/3 \times 64/3 \times 32/3 \times 16/3 \times 8/3 \times 4$	$3 \times 400 + 5 \times 1.5\%$ or $-10 \times 1.5\%$
Rated Primary Current, A	3×33.2	3×33
Rated Secondary Current, A	$3 \times 30/3 \times 30/3 \times 30/3$ $3 \times 30/3 \times 30/3 \times 30$	3×32.5
Rated Power, kVA	22.5	22.5
Rated Frequency, Hz	50	50
Connection Group	D/i iiiii	Yy0
Short-Circuit Voltage, %	3.88	5.10

In the testing setup, the series voltages are incorporated in the transmission line separately, so the regulation of quadrature voltage is applied directly by the proposed ACPST. In HV PST, each series voltage regulation is made by the tap changes on the secondary windings of the transformer (in cases of two core PSTs). However, these differences do not impact the ACPST work in the considered steady states. A connection diagram of the ACPST is presented in Figure 6.

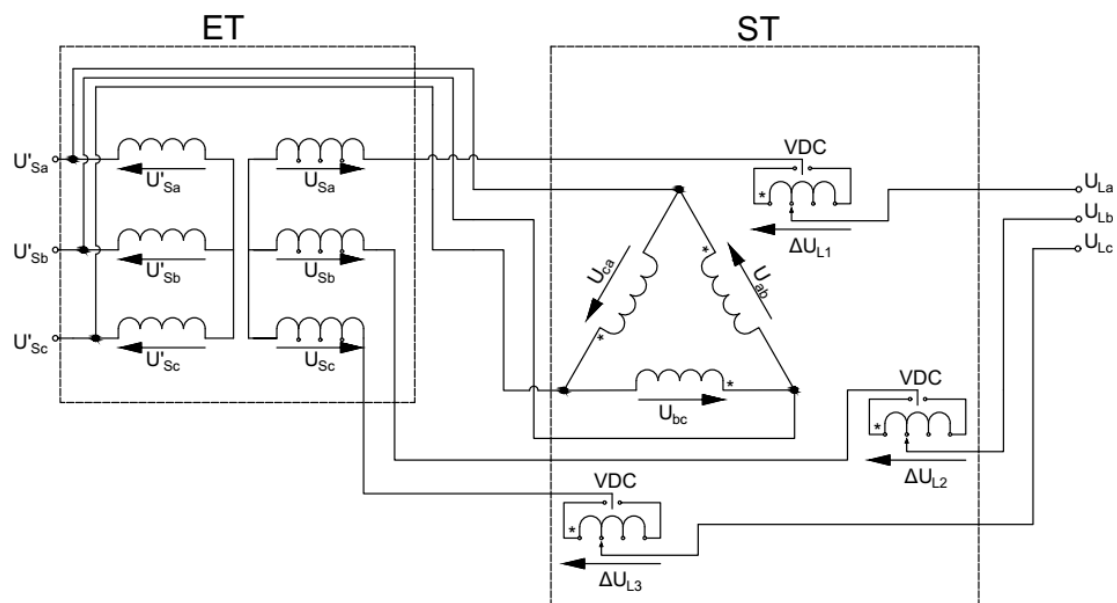


Figure 6. Connection diagram of laboratory ACPST.

Both transformers have individual roles: ET regulates the longitudinal voltage, and ST regulates and injects voltage into the transmission line as additional voltage. Due to both voltages' regulation, it is possible to obtain control strategies, such as asymmetric mode, symmetric mode, constant output voltage value, constant angle and transmission line parameter compensation (as in UPFC or Sen Transformer).

The presented possibilities of ACPST allow for using this device as a flexible power flow control device. This is the thesis that will be examined in this manuscript.

A five-bus power system in the laboratory was arranged according to Figure 7. PST was installed in line L34, and the remaining lines were adjusted to demonstrate its properties [28].

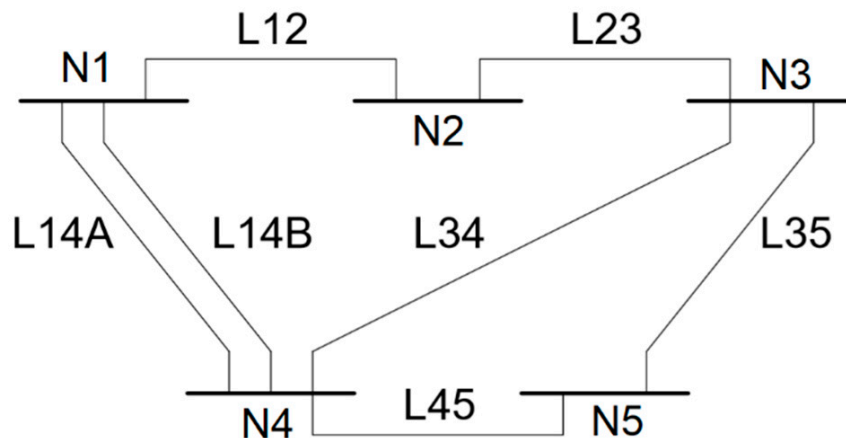


Figure 7. Five-bus laboratory power system—the initial arrangement.

The data acquisition systems consist of current measurement (current clamps—Fluke i1000ac, range 100 A, accuracy 2% ± 5 mV), voltage measurement (voltage probes—Pintek DP200, accuracy: ≤±2%) and measurement card (National Instruments USB-6259 BNC, Austin, TX, USA). The collected data were processed using SignalExpress 2015 and Matlab R2022b software.

3.2. Power Flow Simulations

The simulations were prepared using MatPower [29] for a five-bus IEEE-based system, using a power flow tool with the Newton–Raphson calculation method [30,31].

$$\begin{bmatrix} \Delta P \\ \Delta Q \end{bmatrix} = \begin{bmatrix} H & N \\ M & L \end{bmatrix} \begin{bmatrix} \Delta \delta \\ \Delta U \end{bmatrix} \tag{4}$$

where, H, N, M and L are elements of the Jacobian matrix, given as:

$$[H] = \left[\frac{\partial \Delta P_i}{\partial \Delta \delta_j} \right] \tag{5}$$

$$[N] = \left[\frac{\partial \Delta P_i}{\partial \Delta U_j} \right] \tag{6}$$

$$[M] = \left[\frac{\partial \Delta Q_i}{\partial \Delta \delta_j} \right] \tag{7}$$

$$[L] = \left[\frac{\partial \Delta Q_i}{\partial \Delta U_j} \right] \tag{8}$$

Due to the aim of the article, to show the properties of ACPST, both the small five-bus testing power system and the Newton–Raphson calculation method were chosen. Power losses can be observable in such conditions due to operating properties, with an influence on the power flow regulation.

The data collected after testing the five-bus power are presented in Table 2.

Table 2. Parameters of testing 5-bus power system.

Bus	Bus Type	Power Demanded MVA	Power Generated MVA	Voltage Pu
1	Slack bus	150 + j50	0	1
2	PQ	100 + j40	0	Var
3	PV	90	200 + j75	1.06
4	PQ	180 + j100	0	Var
5	PV	0	360 + j65	1.06

The generator voltage in nodes 3 and 5 is intentionally set as 1.06 pu to achieve increased voltage in the system. Due to this, voltage regulation through ACPST can also be compared with APST.

4. Laboratory Tests

Laboratory tests were performed to present the main idea of the ACPST to determine how the power transfer via system lines can be controlled using longitudinal and transverse voltage regulation.

For the no-load conditions (“0” power flow), three cases were considered to prove the influence of ACPST on voltage parameters (value, angle). They are longitudinal input voltage to series transformer U_S , additional quadrature voltage ΔU and output ACPST voltage U_L waveforms. These waveforms are visible in Figure 8 for ET ratio of voltages 400/376 and 400/340 (and phasor diagrams are depicted in Figure 9).

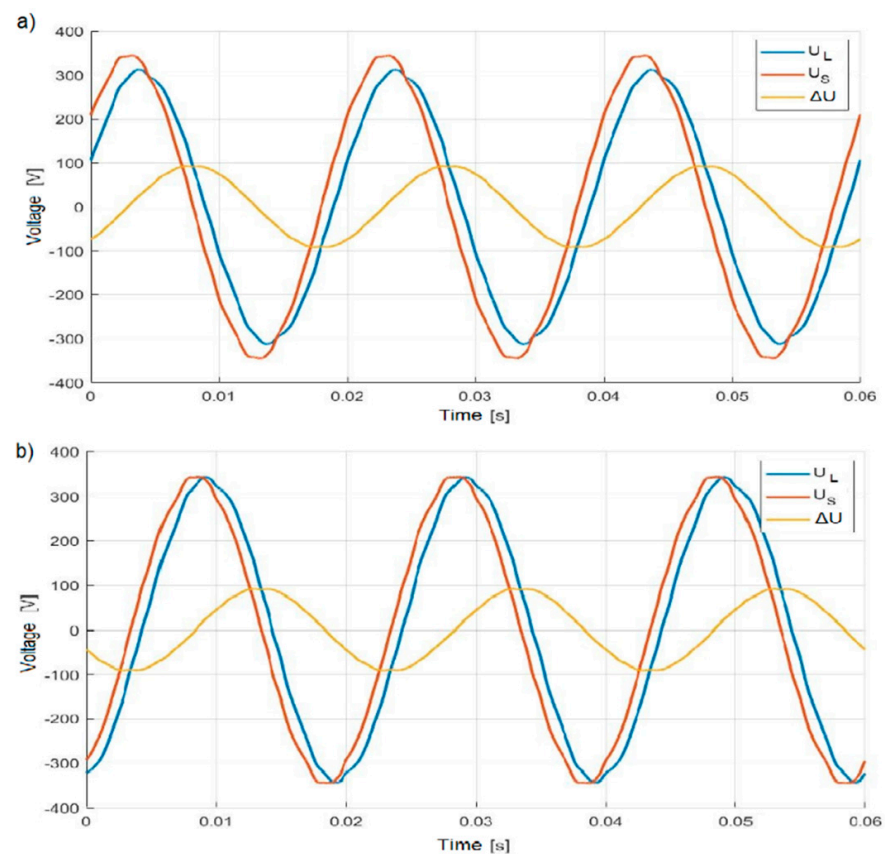


Figure 8. Voltage waveforms for nominal longitudinal voltage (a) and for the lowered one (b) obtained based on a laboratory model.

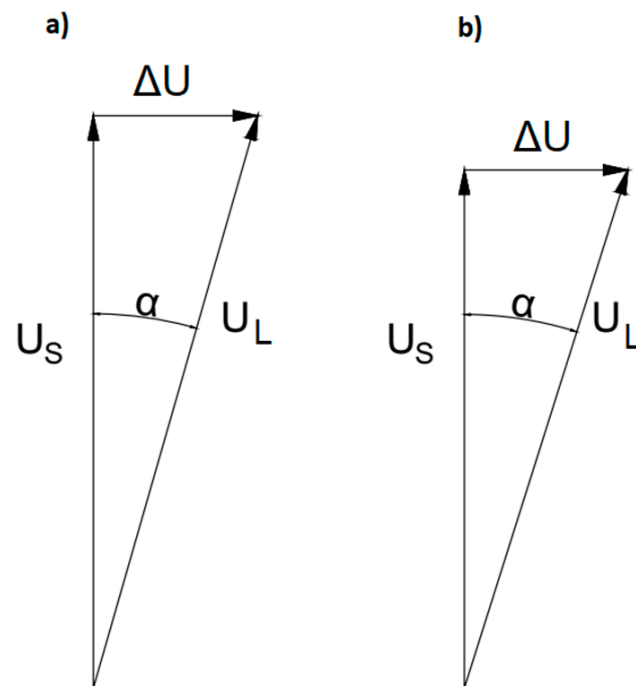


Figure 9. Phasor diagrams for nominal longitudinal voltage (a) and for the lowered one (b).

Based on no-load measurements, phasor diagrams can be drawn for both cases, and voltage parameter values are presented in Table 3.

Table 3. Voltage and angle values for no-load case.

ET Ratio	400/376	400/340
U_S, V	230.3	208.4
$\Delta U, V$	65.8	65.8
U_L, V	239.5	218.5
$\alpha, ^\circ$	-16	-18

No-load condition measurements show that obtaining a higher-angle shift value for lowered longitudinal voltage and the same quadrature one is possible. This ACPST feature allows for a much greater angle shift value for the same output voltage value (for ET ratio of 400/340 to achieve $U_L = 239,5 V$, it should be added $\Delta U = 118 V$ and the angle $\alpha = 30^\circ$).

For the following tests, the authors used a single transmission line connecting two power systems in two longitudinal phase voltage adjustment cases: nominal (230 V) and lowered (196 V). Power transfer is presented in Figure 10.

We observed that active power transfer can be the same for lowered voltage, adding 8 V greater quadrature voltage. Due to this, the exact power equivalent may be transferred with a lower PST output voltage. This is confirmed by the diagram shown in Figure 11, where for the whole range of added voltages and lowered longitudinal voltage, the output voltage is lower than for the nominal one. The voltage varies from 20 V for $\Delta U = 0 V$ to 17 V for $\Delta U = 148 V$.

The conducted tests pointed out that implementing the longitudinal voltage regulation to classic asymmetric PST can efficiently influence voltage parameters to achieve equivalent power transfer. The ACPST properties' validity and utility allow one to conduct power flow calculations in testing a five-bus power system.

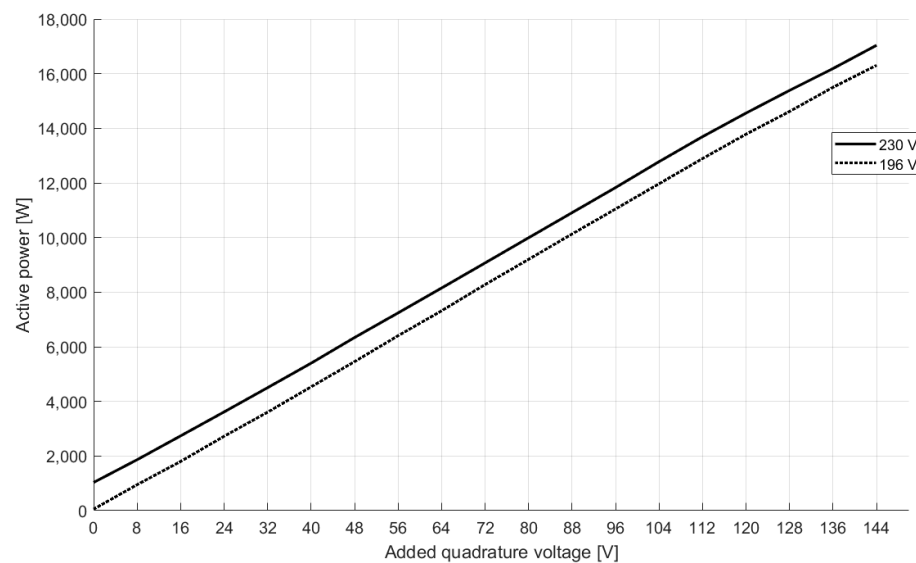


Figure 10. Active power transfer through a single transmission line with installed ACPST connecting two power systems in cases of nominal and lowered longitudinal voltages.

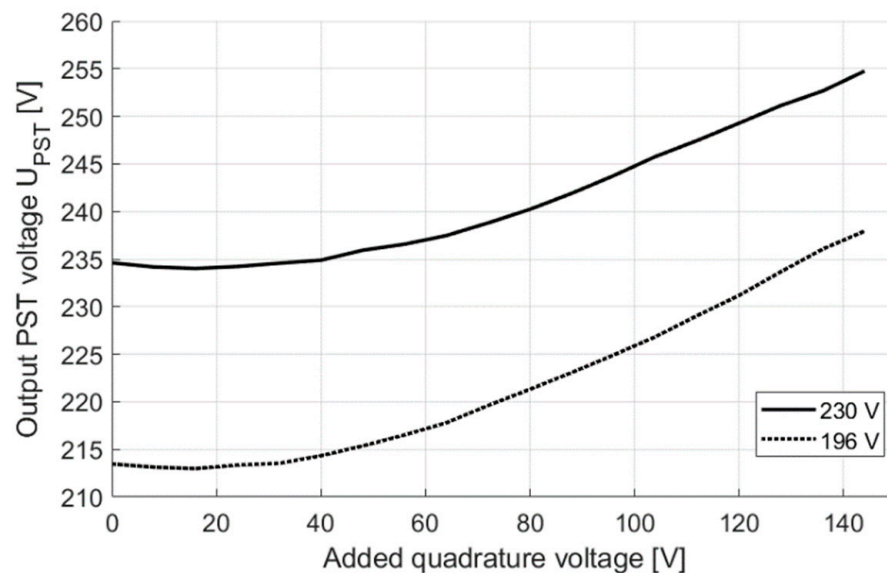


Figure 11. Output PST voltages versus added quadrature voltage in cases of nominal and lowered longitudinal voltages.

5. Power Flow Calculations

Three PST cases will be considered in this section: APST, ACPST working for a constant voltage and ACPST working with lowered longitudinal voltage. In each PST type, the same phase angles will be introduced into the transmission line, and then power flows, bus voltage values, angles and power losses will be analyzed. Assumed phase angles are equal to 5° , 10° and 15° . Each PST is installed in line L45.

The obtained active power values in each line are shown in Figures 12 and 13. In each case, the highest impact on the active power transfer in line L45 is APST, because power transfer was the greatest for the same set phase angle value. The difference in power flows between APST and ACPST with lowered longitudinal voltage is 40 MW less, 50 MW less and 60 MW less in the case of ACPST for set angles 5° , 10° and 15° , respectively. Quasi-symmetric ACPST mode resulted in intermediate active power values between the earlier mentioned cases.

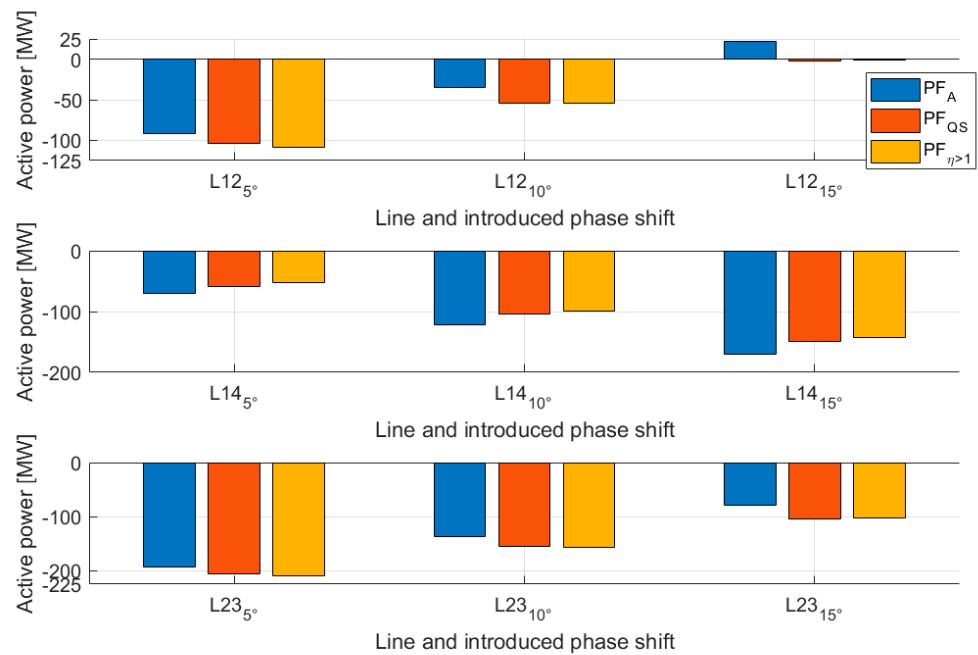


Figure 12. Active power flows in transmission lines for APST (blue), ACPST in quasi-symmetric mode (red), ACPST with lowered longitudinal voltage (yellow).

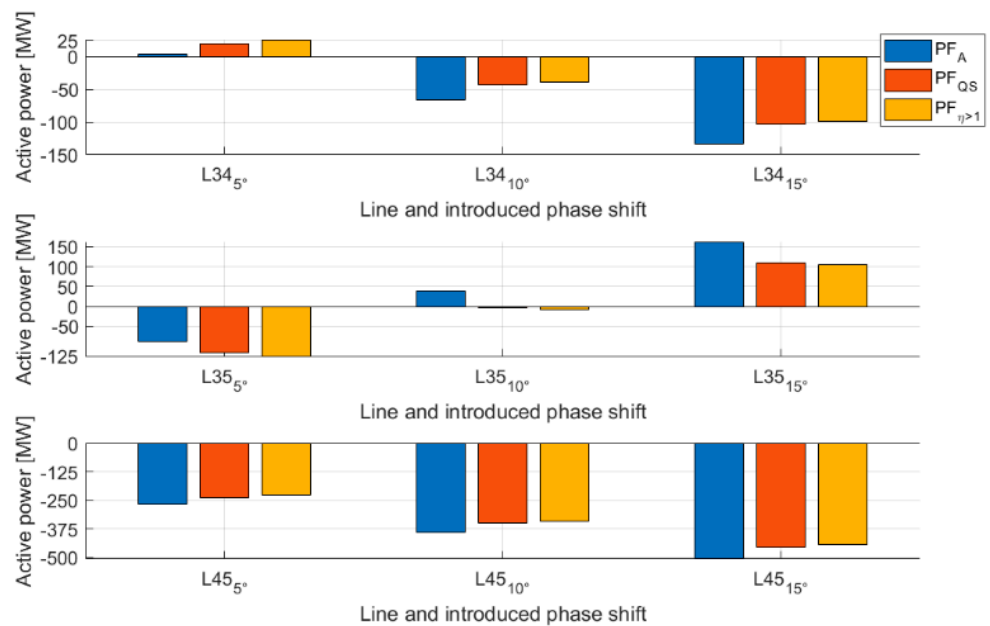


Figure 13. Active power flows in transmission lines for APST (blue), ACPST in quasi-symmetric mode (red), ACPST with lowered longitudinal voltage (yellow).

In Figures 12 and 13, one can see the effect of PST introduction on the power transfer in line L45 and the rest of the system. In some lines, there can be changed power flow direction, e.g., APST and set 15° power flow in L12 is in the opposite direction compared to both ACPST modes (but these values are close to zero). The growing injected voltage, and as a result, phase angle, impacts the power flow changes between considered cases. Line L35, for all PST types, follows dependency: when the set phase angle is low (5°), power flow is from node 3 to node 5, and when this angle is more significant (10° or 15°), the power flow is from node 5 to 3. This is a consequence of the node types (both generation types), and their voltages are set as 1.06 pu. Therefore, the power transmission direction

depends on the relation between phase voltage angles in each bus. For a given angle of 5° voltage vector of bus 5 is before vector 3. In other cases, this relation is changed (for 10° and both ACPST modes, the power flow direction is the same as in the case of angle 5° ; however, the power values are close to zero).

However, active power flows cannot be assumed as the only determiner in the PST's properties analyses. Therefore, voltages in node 4 of the power system model are compared in Table 4.

Table 4. Voltage parameters in node 4.

	Voltage [kV]	Angle [°]	Voltage [kV]	Angle [°]	Voltage [kV]	Angle [°]
Set phase shift	5°		10°		15°	
APST	412.4	1.16	413.2	2.21	414.4	3.17
ACPST QS	411.6	0.94	410.8	1.92	409.2	2.88
ACPST $\eta > 1$	403.2	1.03	403.6	2.02	404.4	2.91

ACPST usage, independently of the chosen control mode, results in lower voltage values in node 4 than in classic APST. For lowered longitudinal voltage and the 400 kV system, the value difference is greater than 9 kV. Such values can affect the extension of the ACPST range of use to achieve more flexible PST control with chosen power flows and nodal voltage values. The highest voltage angle values in each case are noticeable for the APST and the smallest ones for the quasi-symmetric mode.

Due to the differences in active power flows in line L45, achieving the same active power values in line with PST was set as the next calculation objective. This scenario required recalculating setting values of ACPST; however, the obtained results were the same in line L45 with voltage values assembled and presented in Table 5.

Table 5. Voltage parameters in node 4.

	Voltage [kV]	Angle [°]	Voltage [kV]	Angle [°]	Voltage [kV]	Angle [°]
APST	5°		10°		15°	
	412.4	1.16	413.2	2.21	414.4	3.17
ACPST QS	6.2°		12.1°		17.9°	
	411.6	1.19	408.4	2.30	406.0	3.37
ACPT $\eta > 1$	6.6°		12.2°		18°	
	403.2	1.36	403.6	2.43	404.8	3.41

To obtain the same power flows in line L45, in both quasi-symmetric and lowered longitudinal voltage ACPST modes, set phase shift values had to be greater than in the APST case. The highest values are visible for the last case (APST 15°); however, the differences between set angle values are minimal.

It should be mentioned that quasi-symmetric mode causes voltage drops with the set phase shift values. This is a consequence of higher power flows and voltage drops in the lines, while ACPST is controlled to maintain an output voltage value only on the same level as the input one [27].

For the same phase shifts, quasi-symmetric ACPST mode stands out in the lowest active and reactive power losses (see Table 6). However, for the same power flows in L45, higher power losses for ACPST compared to APST are visible. The lowered longitudinal voltage mode results in the highest power losses for 5° , 10° and 15° angles.

Table 6. Active and reactive power losses in the testing 5-bus power system.

	ΔP , MW	ΔQ , MVar	ΔP , MW	ΔQ , MVar	ΔP , MW	ΔQ , MVar
APST	5°		10°		15°	
	8.1	47.8	13.4	83.1	22.2	140.9
ACPST QS	5°		10°		15°	
	7.1	47.3	11.4	77.8	18.4	127.7
	6.2°		12.1°		17.9°	
	7.8	42.9	19.5	95.0	33.1	163.9
ACPST $\eta > 1$	5°		10°		15°	
	8.9	47.2	15.4	76.9	25.8	125.5
	6.6°		12.2°		18°	
	10.7	54.6	19.5	96.0	33.1	163.9

6. Conclusions

The PST structure solution presented in this paper allows for both longitudinal and quadrature voltage regulation and permits flexible control strategies via voltage adjustment dependently on the required objective functions. The asymmetric controllable phase-shifting transformer (ACPST) can be used as a classic asymmetric PST (angle regulation, output voltage growth), power system transformer (voltage regulation) or by connecting both modes to find the chosen mode resulting in decreasing/increasing output voltage, constant voltage value maintaining or even realizing functions as sophisticated as ones performed using UPFC.

The presented results show that adding only 8 V greater quadrature voltage allows the proposed solution to maintain the same power flow, even for the output voltage reduced from the nominal value of 230 V to the value of 196 V.

Laboratory tests were conducted on the two-transformer ACPST unit. Both power flow control and voltage regulation (the value and angle) were possible. The laboratory research confirmed the expected results obtained from the simulation—to maintain constant active power flow when longitudinal voltage was lowered, the angle had to be increased for the same quadrature voltage injection in the line.

The application of the proposed device is not only to control power flow between systems but also to control power flow within power system lines, which can produce optimum power transmission (minimum losses) in the supply system. In the five-node test power system, the power losses with the quasi-symmetric ACPST mode stands are, depending on the controlled phase shift angle, even 12% lower than in the case of the classic APST.

The power flow measurements and simulations were conducted only for continuous steady-state conditions and do not include transient conditions, which occur during changes within power system models (laboratory or simulation in MATLAB) and during changes in the PST voltages. Future research aims to determine the impact of the proposed phase shifter system on the power system dynamics. Work is also planned to attempt to use the shifter to mitigate disturbances in the power system.

Author Contributions: Conceptualization, J.S. and B.R.; methodology, P.A.; software, P.A. and M.S.; validation, J.S., M.S. and B.R.; formal analysis, J.S. and P.C.; investigation, P.A. and B.R.; resources, P.A. and B.R.; writing—original draft preparation, P.A. and J.S.; writing—review and editing, M.S., B.R. and P.C.; visualization, P.A. and B.R.; supervision, M.S., J.S. and P.C.; funding acquisition, M.S. All authors have read and agreed to the published version of the manuscript.

Funding: This research received no external funding.

Conflicts of Interest: The authors declare no conflict of interest.

References

1. Shalukho, A.V.; Lipuzhin, I.A.; Voroshilov, A.A. Power Quality in Microgrids with Distributed Generation. In Proceedings of the 2019 International Ural Conference on Electrical Power Engineering (UralCon), Chelyabinsk, Russia, 1–3 October 2019; pp. 54–58. [\[CrossRef\]](#)
2. Mozina, C.J. Impact of Green Power Distributed Generation. *IEEE Ind. Appl. Mag.* **2010**, *16*, 55–62. [\[CrossRef\]](#)
3. Strezoski, L.; Stefani, I.; Brbaklic, B. Active management of distribution systems with high penetration of distributed energy resources. In Proceedings of the 18th International Conference on Smart Technologies, Novi Sad, Serbia, 1 July 2019; pp. 1–5.
4. Korab, R.; Owczarek, R. Kształtowanie transgranicznych przepływów mocy z wykorzystaniem przesuwników fazowych. *Rynek Energii* **2012**, *5*, 8–15.
5. Bieroński, S.; Korab, R.; Owczarek, R. Wpływ regulacji przesuwników fazowych instalowanych w rejonie Europy Środkowo-Wschodniej na transgraniczne przepływy mocy. *Prace Naukowe Politechniki Śląskiej. Elektryka* **2015**, *61*, 7–22.
6. Verboomen, J.; Van Hertem, D.; Schavemaker, P.H.; Kling, W.L.; Belmans, R. Phase shifting transformers: Principles and applications. In Proceedings of the 2005 International Conference on Future Power Systems, Amsterdam, The Netherlands, 16–18 November 2005; p. 6.
7. Van Hertem, D.; Eriksson, R.; Söder, L.; Ghandhari, M. Coordination of multiple power flow controlling devices in transmission systems. In Proceedings of the 9th IET International Conference on AC and DC Power Transmission (ACDC 2010), London, UK, 19–21 October 2010; pp. 1–6. [\[CrossRef\]](#)
8. Bresesti, P.; Sforna, M.; Allegranza, V.; Canever, D.; Vailati, R. Application of phase shifting transformers for a secure and efficient operation of the interconnection corridors. In Proceedings of the IEEE Power Engineering Society General Meeting, Denver, CO, USA, 6–10 June 2004; Volume 2, pp. 1192–1197. [\[CrossRef\]](#)
9. Morrell, T.J.; Eggebraaten, J.G. Applications for Phase-Shifting Transformers in Rural Power Systems. In Proceedings of the 2019 IEEE Rural Electric Power Conference (REPC), Bloomington, MN, USA, 28 April–1 May 2019; pp. 70–74. [\[CrossRef\]](#)
10. Schmidt, T. ABB AG Transformers. In *Phase-Shifting Transformers Applications and Technology*; ABB Group, 2016.
11. ENTSO-E. Regional Investment Plan CCE. In *Draft Version Prior to Public Consultation*; ENTSOE: Brussel, Belgium, 2020.
12. Polster, S.; Renner, R. Generalisation of the Line Outage Distribution Factors on Phase Shifting Transformers. In Proceedings of the 53rd International Universities Power Engineering Conference (UPEC), Glasgow, UK, 4–7 September 2018; pp. 1–6. [\[CrossRef\]](#)
13. Sosnina, E.; Loskutov, A.; Asabin, A.; Bedretdinov, R.; Kryukov, E. Power flow control device prototype tests. In Proceedings of the 2016 IEEE Innovative Smart Grid Technologies—Asia (ISGT-Asia), Melbourne, VIC, Australia, 28 November–1 December 2016; pp. 312–316. [\[CrossRef\]](#)
14. McMillan, B.; Guido, P.; Leitermann, O.; Martinelli, V.; Gonzaga, A.; McFetridge, R. Application of Power Electronics LV Power Regulators in a Utility Distribution System. In Proceedings of the 2015 IEEE Rural Electric Power Conference, Asheville, NC, USA, 19–21 April 2015; pp. 43–47. [\[CrossRef\]](#)
15. Hadzimuratovic, S.; Fickert, L. Determination of critical factors for optimal positioning of Phase-Shift Transformers in interconnected systems. In Proceedings of the 19th International Scientific Conference on Electric Power Engineering (EPE), Brno, Czech Republic, 16–18 May 2018; pp. 1–6. [\[CrossRef\]](#)
16. Brilinskii, A.S.; Badura, M.A.; Evdokunin, G.A.; Chudny, V.S.; Mingazov, R.I. Phase-Shifting Transformer Application for Dynamic Stability Enhancement of Electric Power Stations Generators. In Proceedings of the IEEE Conference of Russian Young Researchers in Electrical and Electronic Engineering (EIConRus), St. Petersburg/Moscow, Russia, 27–30 January 2020; pp. 1176–1178. [\[CrossRef\]](#)
17. Ding, T.; Bo, R.; Bie, Z.; Wang, X. Optimal selection of phase shifting transformer adjustment in optimal power flow. *IEEE Trans. Power Syst.* **2017**, *32*, 2464–2465. [\[CrossRef\]](#)
18. Korab, R.; Połomski, M.; Owczarek, R. Application of particle swarm optimization for optimal setting of Phase Shifting Transformers to minimize unscheduled active power flows. *Appl. Soft Comput.* **2021**, *105*, 107243. [\[CrossRef\]](#)
19. Ashpazi, M.A.; Mohammadi-Ivatloo, B.; Zare, K.; Abapour, M. Probabilistic allocation of thyristor-controlled phase shifting transformer for transient stability enhancement of electric power system. *IETE J. Res.* **2015**, *61*, 382–391. [\[CrossRef\]](#)
20. Albrechtowicz, P.; Szczepanik, J. The Comparative Analysis of Phase Shifting Transformers. *Energies* **2021**, *14*, 4347. [\[CrossRef\]](#)
21. Ziemianek, S. Model matematyczny zespołu transformatorowego z trapezoidalnym zakresem regulacji przekładni zespolonej do analiz ustalonych i quasi-ustalonych stanów pracy symetrycznych fazowo. *Przegląd Elektrotech.* **2013**, *89*, 143–151.
22. Sen, K.K.; Sen, M.L. Comparison of the Sen transformer with the unified power flow controller. *IEEE Trans. Power Deliv.* **2003**, *18*, 1523–1533. [\[CrossRef\]](#)
23. Sen, K.K.; Sen, M.L. Versatile Power Flow Transformers for Compensating Power Flow in a Transmission Line. Patent No. US6420856B1, 16 July 2002.
24. Sen, K.K.; Sen, M.L. Versatile Power Flow Transformers for Compensating Power Flow in a Transmission Line. Patent No. US6384581B1, 7 May 2002.
25. Machowski, J.; Lubośny, Z. *Stabilność Systemu Elektroenergetycznego*; Wydawnictwo WNT: Warsaw, Poland, 2018.
26. Żurek, S.; Przygodzki, M. The Use of a Regulating Transformer for Shaping Power Flow in the Power System. *Energies* **2023**, *16*, 1548. [\[CrossRef\]](#)

27. Albrechtowicz, P. Phase-Shifting Transformer Efficiency Analysis Based on Low-Voltage Laboratory Units. *Energies* **2021**, *14*, 5049. [[CrossRef](#)]
28. Szczepanik, J.; Rozegnał, B. The development of the real life model of the five node power system, *Czasopismo Techniczne. Elektrotechnika* **2015**, *112*, 83–102.
29. Zimmerman, R.D.; Murillo-Sanchez, C.E. *MATPOWER User's Manual*; Version 7.1; 2020. [[CrossRef](#)]
30. Machowski, J. *Regulacja Systemu Elektroenergetycznego*; Oficyna Wydawnicza Politechniki Warszawskiej: Warsaw, Poland, 2017.
31. Kanicki, A. Systemy Elektroenergetyczne. Available online: <http://www.ssdservice.pl/FTPserwer/ELEKTROTECHNIKA/systemy/systemy%20roz.%203.pdf> (accessed on 22 March 2022).

Disclaimer/Publisher's Note: The statements, opinions and data contained in all publications are solely those of the individual author(s) and contributor(s) and not of MDPI and/or the editor(s). MDPI and/or the editor(s) disclaim responsibility for any injury to people or property resulting from any ideas, methods, instructions or products referred to in the content.